

Interacting quantum box superlattice by self-organized Co nanodots on Au(788)

C. Didiot,¹ A. Tejada,² Y. Fagot-Revurat,¹ V. Repain,² B. Kierren,¹ S. Rousset,² and D. Malterre¹

¹Laboratoire de Physique des Matériaux, Université Henri Poincaré, Nancy I, B.P. 239, 54506 Vandoeuvre-lès-Nancy, France

²Laboratoire Matériaux et Phénomènes Quantiques, CNRS, Université Paris Diderot, B.P. 7021, 75205 Paris, France

(Received 29 May 2007; published 23 August 2007)

Noble metals exhibit a Shockley state that can be confined in one direction due to the interaction with steps in vicinal surfaces. We observe here that self-organized Co islands on Au(788) can also confine the surface state to the orthogonal direction. The two-dimensional confinement of the surface state is studied by scanning tunneling spectroscopy as well as photoemission. Several confined states are revealed by the standing-wave pattern which appears between the Co nanodots. The band dispersion shows the opening of three gaps. These gaps report on the magnitude of the surface potential, which is drastically different from that of the Au substrate. These results show how self-organization modulates the electronic potential, leading to a periodical confinement of the surface state.

DOI: [10.1103/PhysRevB.76.081404](https://doi.org/10.1103/PhysRevB.76.081404)

PACS number(s): 73.21.Cd, 79.60.Jv, 79.60.-i, 68.37.Ef

Tailoring electronic states in nanostructures presents both fundamental and technological interest. Quantum size effects control the lasing properties in complex structures^{1,2} or trigger novel phenomena in low dimensions: oscillatory magnetic coupling,³ structural transitions,^{4,5} spin-charge separation in Luttinger liquids,⁶ oscillation of the superconducting temperature,^{7,8} etc. Noble-metal (111) surfaces are particularly suitable for exploring low-dimensional physics, since they display a Shockley surface state easily affected by changes in the surface structure. One-dimensional (1D) surface superstructures have revealed very successful to drive 2D systems towards 1D electronic confinement. This transition appears, for instance, in metallic vicinal surfaces,⁹⁻¹² periodically faceted surfaces,^{13,14} and epitaxial Ag films deposited on reconstructed Si(111) surfaces¹⁵ or adsorbate-induced striped Cu-O surfaces.¹⁶ Although electronic quantum behavior is generally taken as a fact, confinement in nanopatterned surfaces has been rarely reported. Very recently 0D confinement has been observed in molecular gratings.¹⁷ In this work, we demonstrate how self-organization on Au vicinal surfaces leads to an assembly of quantum boxes.

Noble metals exhibit a free-electron-like surface state on the close-packed (111) faces located at the last monolayers and are therefore very sensitive to the surface potential. Structural modifications have been demonstrated to affect the surface-state properties. In particular, it has been shown that the Shockley state can be confined to a variety of natural or artificial nanostructures.¹⁸⁻²³ These quantum systems are experimental manifestations of the “particle in a box” problem of quantum mechanics. Among these systems, vicinal surfaces play an important role in tailoring the surface electronic properties.¹⁰⁻¹² Steps can lead either to superlattice zone folding in narrow terraces or to 1D confinement in larger terraces.^{11,12}

The Au(788) vicinal surface is a regular array of (111)-oriented terraces of 38 Å width which can be used as a template to grow self-organized Co cluster lattices. When the growth of Co is adequately performed, self-organization is achieved and a Co array is found. The Co lattice is stable even at room temperature, and the ordering is highly homogeneous over the sample. The homogeneity of the structural

properties in this self-organized system allows us to apply spatially averaging techniques.^{24,25} We have employed both angular-resolved photoemission spectroscopy (ARPES) and scanning tunneling microscopy and spectroscopy (STM and STS) to study the electron confinement among Co islands on the vicinal substrate Au(788). A partial confinement is obtained due to the interaction of steps and unconnected Co islands with the surface state.

The single-crystal surface was prepared through cycles of Ar-ion sputtering and annealed at 700 K afterwards. Co was first evaporated at 150 K and then annealed at room temperature. The STM and STS measurements were performed in a LT-STM Omicron coupled to a photoemission chamber, where the sample is transferred without breaking the ultrahigh-vacuum conditions. Differential tunnel conductance images were acquired with a PtIr tip under a bias modulation of 10 mV at 700 Hz and a lock-in detection of the tunnel current. Conductance maps dI/dV were recorded in closed feedback loop conditions. The STM images were analyzed with the WSXM package.²⁶ Photoemission experiments were performed with a high-resolution Scienta SES 200 spectrometer equipped with angle and energy multidection and He I radiation from a discharge lamp. ARPES spectra were taken with energy resolution $\Delta E \sim 5$ meV and angular resolution $\Delta\theta \sim 0.3^\circ$.

Figure 1(a) shows a topographic STM image of 0.40 ML Co on Au(788). Au(788) exhibits a rectangular lattice of preferential adsorption centers at the intersection of the gold discommensuration lines and step edges.²⁷ As a consequence of the nucleation process at preferential sites, a rectangular lattice of Co clusters is obtained with long-range order. The unit cell can be defined from the four Co clusters at the corners [inset of Fig. 1(a)], whose size is $=3.8 \times 7.2$ nm². This unit cell is determined in one direction by the width of terraces (L_x) and in the orthogonal one by the periodicity of the discommensuration lines, naturally lying on the terraces (L_y). The differential conductance (dI/dV) is shown for different bias voltages in Fig. 1(b). In between the Co islands, spatial modulations are clearly evidenced in the local density of states (LDOS) of the surface, with nodes and maxima depending on the bias voltage. At $V = -375$ mV, a

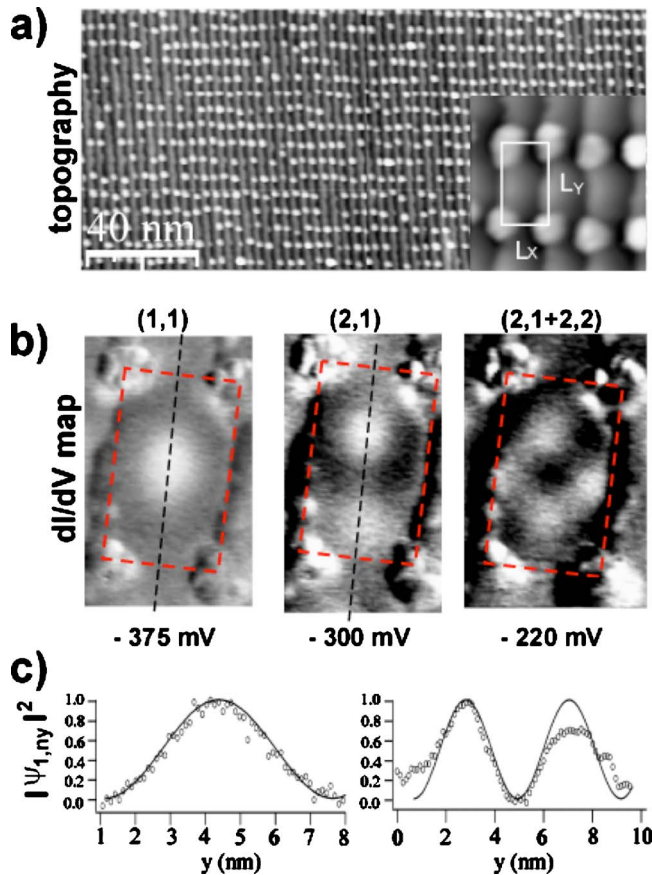


FIG. 1. (Color online) (a) Topographic STM image of 0.4 ML Co/Au(788). The inset shows a detail of several unit cells, each one delimited by four Co dots at the intersections of the gold reconstruction and the step edges. (b) Differential conductance maps dI/dV at $T=80$ K for different bias voltages. The dotted rectangle on the maps indicates the unit cell. (c) Comparison between experimental cuts along the dotted lines in (b) and the LDOS within a hard well model. The resonance (1,1) is fitted with $L_y=5.5$ nm and the (2,1) resonance with $L_y=6.0$ nm.

single maximum in the center of the box is observed. When increasing the bias voltage to -300 mV, two different maxima appear around a central node along the y direction. Finally, at $V=-220$ mV, two additional maxima appear along the x direction. The LDOS has therefore nodes at the step edges and between the Co islands. This behavior suggests that, in addition to the repulsive barrier at step edges,^{10–12} an additional barrier is created by the unconnected Co islands. The box delimited by the four Co dots acts thus similarly to a quantum box for Shockley states, leading to a standing-wave pattern in the different unit cells [Fig. 2(a)]. As expected, maxima in the LDOS appear only for bias voltages above the band edge of the Au(111) surface-state electrons ($E_0=-460$ meV).^{10,28} All of these phenomena, which are absent in the clean surface, suggest confinement induced by the Co dots.

In order to roughly describe the LDOS, we have considered full confinement perpendicular to the steps¹⁰ and also a hard-wall model with effective width L_y along them. However, it is impossible to find an L_y independent of the energy

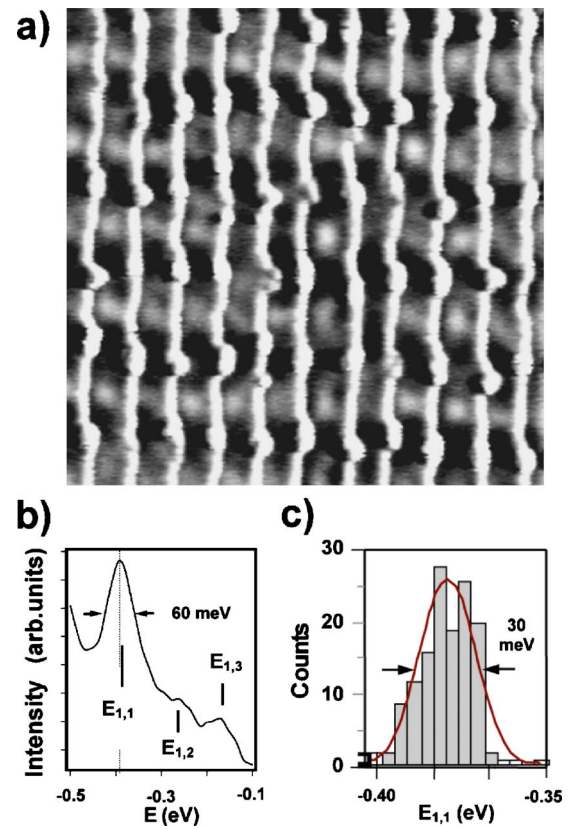


FIG. 2. (Color online) (a) Differential conductance map (30×30 nm², $T=5$ K) at a bias voltage of -395 mV, which corresponds to the fundamental mode energy. (b) LDOS measured by STS over the center of a single quantum box (averaging on a rectangle of 0.5×1 nm²). The averaging improves the signal-to-noise ratio without affecting the spectral width. (c) Histogram of the fundamental mode energy measured by STS in 128 unit cells.

that describes simultaneously the energy and the spatial distribution of the modes. In order to correctly describe the spatial distribution of the LDOS, L_y needs to be increased with energy while it should remain constant [Fig. 1(c)]. The energetic dependence points towards a partial transmission across the barrier created between the unconnected Co islands. Transmission effects can be quantified by considering the energetic spectral width of the resonances. The dI/dV spectrum at the center of the unit cell [Fig. 2(b)] shows a low-energy resonance $E_{1,1}=-395$ mV (labeled by the quantum numbers n_x and n_y) with a spectral width of 60 meV. Two additional broad peaks are observed at higher energies ($E_{1,2}$ and $E_{1,3}$). It has been shown that in the case of multiple scattering of electron waves in quantum boxes, the broadening mechanisms are usually dominated by a reflection coefficient lower than unity, the nonreflected part being absorbed or scattered into bulk states.²⁹ Intrinsic effects like electron-electron and electron-phonon interactions can also contribute. For instance, in Fe/Cu(111) quantum corrals,¹⁸ the theoretical description has shown that only 25% of the surface-state electrons are reflected at the corral, whereas 50% are absorbed into bulk states.³⁰ The observed spectral width in these corrals is ~ 30 meV, while in our case, the spectral

width of $E_{1,1}$ is twice this value, so transmission must play a role. Self-organized Co nanodots on Au(788) cannot thus be accurately described by an infinite-well model.

A better description must take into account the partial transmission along the direction parallel to the steps. In the following, we will focus on the dispersion along this direction. The gaps in the surface-state band due to the potential V created by the Co islands are related to the V_{Gn} Fourier components of the potential:

$$V = \sum_{n=1}^{\infty} V_{Gn} \cos\left(\frac{2\pi y}{L_y} n\right). \quad (1)$$

Figure 2(a) shows a dI/dV map at $V=-395$ meV, where the lowest-energy resonance $E_{1,1}$ appears at every unit cell. The resonance intensity varies according to variations in the quantum box size and shape, which displace the energy of the resonances. The histogram of the energy of $E_{1,1}$ peak at different unit cells [Fig. 2(c)] gives an average energy $\langle E_{1,1} \rangle = -360$ meV with a standard deviation of 30 meV. Since the standard distribution is smaller than the spectral width of the peak, photoemission provides valuable information when studying the gaps in the surface bands.

ARPES can properly study this homogeneous self-organized system. Figure 3 shows the photoemission data for the dispersion along the steps on the clean surface and on Co/Au(788). Panels (a) and (b) present the second derivative of the photoemission spectra. The data resolution allows one to observe on the clean surface [Fig. 3(a)] the spin-orbit-split band of the Shockley state.^{31,32} Moreover, it is possible to observe the tiny gaps induced by the Au reconstruction on the clean surface.³³ These gaps appear in the region where the band centered at $k=0$ crosses the bands originating from the reconstruction periodicity and centered at $n\pi/L_y$. On Co/Au(788), the dispersion relation [Fig. 3(b)] corresponds to a gapped parabola. Owing to the geometry of the detection that selects $k_x=0$, all these resonances are associated with the first-quantized state in the direction perpendicular to the step ($n_x=1$). The resonances can thus be labeled with the quantum numbers n_x and n_y associated with both directions: $E_{1,1}=-370$ meV, $E_{1,2}=-280$ meV, $E_{1,3}=-180$ meV, and $E_{1,4}=-50$ meV. The energetic position agrees reasonably well with the STS ones observed in the dI/dV images and spectra. The resonances are delimited by the gaps that appear at the same energies as on the clean surface [see the dotted lines in Figs. 3(a) and 3(b)]. The reason is that self-organized Co dots appear with the same periodicity of the reconstruction. However, the gaps in the self-organized surface are clearly magnified when compared to the substrate, indicating a stronger potential for surface electrons. A clear example is given in Figs. 3(d) and 3(e). These panels compare the region of the third gap around -150 meV for both the clean and the self-organized surfaces. Dotted lines are guides for the eye to indicate the dispersion of the spin-orbit-split band and the gap opening. The gap is defined by the highlighted spectrum, which corresponds to the distance between the maximum of the highest binding energy branch and the minimum of the lowest binding energy branch. The third gap in the self-organized system is more than 4 times larger than on the

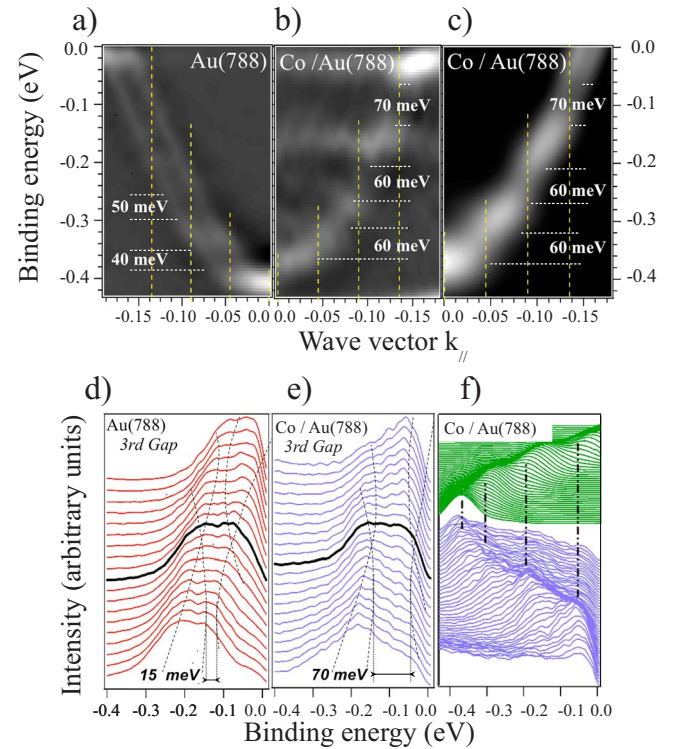


FIG. 3. (Color online) (a) Second derivative in gray scale of the ARPES spectra at the substrate Au(788) and (b) of self-organized Co islands on Au(788). Bright colors mean more intensity. Four maxima corresponding to the confinement are observed when Co islands are present. The dotted lines show the position of the gaps. The magnitude of the gaps are also indicated. (d) Energy dispersion curves (EDCs) around the third gap on the Au(788) substrate. (e) EDCs around the third gap on self-organized Co islands on Au(788). (f) Comparison between simulated photoemission EDCs (upper part of the panel) and experimental spectra (lower part).

clean surface. The widening of the other gaps can also be observed in Figs. 3(a) and 3(b). These data show unambiguously that Co dots strengthen the periodic potential of the surface, leading to clear resonances in the self-organized system. The simulation of the ARPES spectra reproduces the experimental gaps. Therefore, it is possible to estimate V_{Gn} . By diagonalizing the Hamiltonian of an electron with a given kinetic energy in the presence of a periodical potential, $E(k)$ and its spectral weight can be calculated. Then, the simulation of the photoemission spectra needs the introduction of a finite resolution and the conversion from k to θ . In this way, the experimental gaps can be reproduced for different values of the Fourier components of the potential. Although the phase of the components cannot be determined by photoemission and this procedure may not have a unique solution, reasonable assumptions to reduce the number of possibilities can be performed. In particular, STM points towards a minimum in the potential in the unit cell center [Fig. 1(b), left panel]. The edges of the unit cell repel electrons due to the negligible LDOS between Co islands, so the potential must be maximum there. Therefore, in order to reproduce the experimental gaps, we propose $2V_{G1}=80$ meV, $2V_{G2}=60$ meV, and $2V_{G3}=50$ meV. When these values are con-

sidered, the simulated photoemission spectra agree satisfactorily with the experimental EDCs [Fig. 3(f)]. The positions of the resonances and the magnitudes of the gaps are well described. Minor discrepancies appear around -165 meV. At this energy, there is some unexpected spectral weight for a variety of k 's. Such a nondispersive behavior is difficult to explain within the previous model. This feature can reflect the hybridization of the Au s - p state with Co d states in the region of the Co islands, already observed in Co/Au(111) around -150 meV.³⁴ Finally, the experimental photoemission features are adequately understood and our model of the surface potential describes the essential physics at the spectra. The potential is roughly maximum in a small region between Co islands and minimum at the fcc region of the surface. We speculate that the origin of the surface potential in Co/Au(788) can be the strain, since there is a 14.5% lattice mismatch between Co and Au. We cannot also discard the influence of hybridization effects between Co and Au, which must necessarily modify the LDOS near the islands.

In conclusion, we have shown by ARPES and STS that

the free-electron-like dispersion of Shockley states can be modified by a regular lattice of Co nanodots obtained by self-organized growth on Au(788). In addition to the step-edge repulsive barrier, Co islands introduce a surface potential that breaks up clearly the surface-state band into four occupied minibands. The photoemission analysis of the gaps has allowed us to determine the surface potential in the periodic system. Transmission is present between the different unit cells, so the confinement is partial and the quantum boxes are interacting. The Co potential controls the degree of confinement in the quantum boxes, as well as the energy levels. By choosing other substrates or other adsorbed elements or molecules, it will be possible to further tune the electronic properties, opening a new way to manipulate the nanometer scale.

We thank L. Moreau for technical assistance. A.T. acknowledges financial support from GDR Relax for part of the experiments.

- ¹R. Nötzel, Z. Niu, M. Ramsteimer, H. Schönherr, A. Trempert, L. Däweritz, and K. Ploog, *Nature (London)* **392**, 56 (1998).
- ²J. Faist, F. Capasso, D. Sivco, C. Sirtori, A. Hutchinson, and A. Cho, *Science* **264**, 553 (1994).
- ³F. J. Himpsel, J. E. Ortega, G. J. Mankey, and R. F. Willis, *Adv. Phys.* **47**, 511 (1998).
- ⁴Z. Zhang, Q. Niu, and C. K. Shih, *Phys. Rev. Lett.* **80**, 5381 (1998).
- ⁵P. Czoschke, H. Hong, L. Basile, and T.-C. Chiang, *Phys. Rev. Lett.* **91**, 226801 (2003).
- ⁶J. Voit, *Rep. Prog. Phys.* **58**, 977 (1995).
- ⁷Y. Guo, Y. Zhang, X. Bao, T. Han, Z. Tang, L. Zhang, W. Zhu, E. G. Wang, Q. Niu, Z. Q. Qiu, J. Jia, Z. Zhao, and Q. Xue, *Science* **306**, 1915 (2004).
- ⁸T. Chiang, *Science* **306**, 1900 (2004).
- ⁹F. Baumberger, T. Greber, and J. Osterwalder, *Phys. Rev. B* **62**, 15431 (2000).
- ¹⁰A. Mugarza, A. Mascaraque, V. Pérez-Dieste, V. Repain, S. Rousset, F. J. Garcia de Abajo, and J. E. Ortega, *Phys. Rev. Lett.* **87**, 107601 (2001).
- ¹¹J. E. Ortega, A. Mugarza, V. Repain, S. Rousset, V. Pérez-Dieste, and A. Mascaraque, *Phys. Rev. B* **65**, 165413 (2002).
- ¹²A. Mugarza, A. Mascaraque, V. Repain, S. Rousset, K. N. Altmann, F. J. Himpsel, Y. M. Koroteev, E. V. Chulkov, F. J. Garcia de Abajo, and J. E. Ortega, *Phys. Rev. B* **66**, 245419 (2002).
- ¹³J. Lobo, E. G. Michel, A. R. Bachmann, S. Speller, J. Kuntze, and J. E. Ortega, *Phys. Rev. Lett.* **93**, 137602 (2004).
- ¹⁴J. E. Ortega, S. Speller, A. R. Bachmann, A. Mascaraque, E. G. Michel, A. Närmann, A. Mugarza, A. Rubio, and F. Himpsel, *Phys. Rev. Lett.* **84**, 6110 (2000).
- ¹⁵N. Nagamura, I. Matsuda, N. Miyata, T. Hirahara, S. Hasegawa, and T. Uchihashi, *Phys. Rev. Lett.* **96**, 256801 (2006).
- ¹⁶K. Berge, A. Gerlach, G. Meister, A. Goldmann, and E. Bertel, *Phys. Rev. B* **70**, 155303 (2004).
- ¹⁷Y. Pennec, W. Auwärter, A. Schiffrin, A. Weber-Bargioni, A. Riemann, and J. V. Barth, *Nat. Nanotechnol.* **2**, 99 (2007).
- ¹⁸M. Crommie, C. Lutz, and D. Eigler, *Nature (London)* **363**, 524 (1993); *Science* **262**, 218 (1993).
- ¹⁹Y. Hasegawa and P. Avouris, *Phys. Rev. Lett.* **71**, 1071 (1993).
- ²⁰P. Avouris and I.-W. Lyo, *Science* **264**, 942 (1994).
- ²¹A. Bendounan, Y. Fagot-Revurat, B. Kierren, F. Bertran, V. Y. Yurov, and D. Malterre, *Surf. Sci.* **496**, L43 (2002).
- ²²T. Andreev, I. Barke, and H. Hövel, *Phys. Rev. B* **70**, 205426 (2004).
- ²³L. Bürgi, O. Jeandupeux, A. Hirstein, H. Brune, and K. Kern, *Phys. Rev. Lett.* **81**, 5370 (1998).
- ²⁴S. Rohart, V. Repain, A. Tejada, P. Ohresser, F. Scheurer, P. Bencok, J. Ferré, and S. Rousset, *Phys. Rev. B* **73**, 165412 (2006).
- ²⁵N. Weiss, T. Cren, M. Eppe, S. Rusponi, G. Baudot, S. Rohart, A. Tejada, V. Repain, S. Rousset, P. Ohresser, F. Scheurer, P. Bencok, and H. Brune, *Phys. Rev. Lett.* **95**, 157204 (2005).
- ²⁶I. Horcas, R. Fernandez, J. Gomez-Rodriguez, J. Colchero, J. Gomez-Herrero, and A. Baro, *Rev. Sci. Instrum.* **78**, 013705 (2007).
- ²⁷V. Repain, S. Rohart, Y. Girard, A. Tejada, and S. Rousset, *J. Phys.: Condens. Matter* **18**, S17 (2006); V. Repain, G. Baudot, H. Ellmer, and S. Rousset, *Europhys. Lett.* **58**, 730 (2002).
- ²⁸R. Paniago, R. Matdorf, G. Meister, and A. Goldmann, *Surf. Sci.* **336**, 113 (1995).
- ²⁹G. Fiete and E. Heller, *Rev. Mod. Phys.* **75**, 933 (2003).
- ³⁰E. Heller, M. Crommie, C. Lutz, and D. Eigler, *Nature (London)* **369**, 464 (1994).
- ³¹G. Nicolay, F. Reinert, S. Hüfner, and P. Blaha, *Phys. Rev. B* **65**, 033407 (2001).
- ³²S. LaShell, B. A. McDougall, and E. Jensen, *Phys. Rev. Lett.* **77**, 3419 (1996).
- ³³C. Didiot, Y. Fagot-Revurat, S. Pons, B. Kierren, C. Chatelain, and D. Malterre, *Phys. Rev. B* **74**, 081404(R) (2006).
- ³⁴M. V. Rastei, J. P. Bucher, P. A. Ignatiev, V. S. Stepanyuk, and P. Bruno, *Phys. Rev. B* **75**, 045436 (2007).